© 1998 The Chemical Society of Japan Bull. Chem. Soc. Jpn., 71, 2359—2363 (1998) 2359

Potential Sweep Voltammetry of Ion-Transfer at Liquid/Liquid Interface with Preceding Chemical Reaction. Determination of the Rate and Equilibrium Constants from Voltammetric Curves

Hajime Katano* and **Mitsugi Senda**

Department of Bioscience, Fukui Prefectural University, Matsuoka-cho, Fukui 910-1195

(Received May 6, 1998)

The behavior of potential sweep voltammograms for the ion-transfer across the liquid/liquid interface with preceding chemical reactions is discussed. The theoretical results are expressed in the form of the working curves for the peak current, peak potential, and half-peak potential as a function of the kinetic-current parameter, which contains the rate and equilibrium constants of the preceding chemical reaction and the rate of the potential sweep. The working curves are applied to analyze the voltammograms for the transfer of Pb^{2+} ion to nitrobenzene facilitated by 1,4,7,10,13,16-hexathiacyclooctadecane present in nitrobenzene from aqueous medium containing citrate^{3-} ion. The dissociation and association rate constants and the formation constant of Pb^{2+}–citrate^{3-} complex in W-phase are 4.5×10^{4} s^{-1} and 8.0×10^{10} M^{-1} s^{-1} and $10^{6.3}$ M, respectively.

In a previous paper,[1)] it has been shown that the transfer of heavy metal ions, such as Pb^{2+}, Cd^{2+}, and Cu^{2+} ions, across the liquid/liquid or oil/water (O/W) interface facilitated by macrocyclic polythiaether 1,4,7,10,13,16-hexathiacyclooctadecane (HTCO) present in O-phase can be studied using cyclic voltammetry and pulse voltammetry. The voltammetric behavior of the facilitated transfer of, for example, Pb^{2+} ion can be explained by the theoretical equations of reversible voltammograms in which both the rate of the ion-transfer across the O/W interface and those of the dissociation and association reaction of the metal ion complexes with ionophores in O-phase and with hydrophilic ligands in W-phase are assumed to be sufficiently rapid compared with the rates of the mass transfer (diffusion) in the two phases. Thus, the ion-transfer voltammetry can advantageously be applied to the study of stoichiometry and/or formation constants of the metal ion complexes in the two phases.[1,2)] It was found, however, that under certain conditions when the formation of metal ion complexes in W-phase is shifted largely to the complex side, the voltammograms of the facilitated ion-transfer were not exactly explained by the equations of reversible voltammograms; rather certain kinetic effects were observed in their behavior.[3)]

In this paper, the behavior of potential sweep voltammograms for the ion-transfer with preceding chemical reactions (for a general review, see Ref. 4) is discussed. The ion-transfer mechanism may also be applied to analyze the facilitated ion-transfer across the O/W interface according to the CE-mechanism[5)] under certain conditions. The mathematical problem of the potential sweep voltammetry of the electrode process coupled with preceding chemical reaction has been solved first by Nicholson and Shain[6)] and discussed in further details by Savéant and Xu.[7)] Recently, a digital simulation technique has also been applied to this problem.[8)] In the present study, by following Nicholson-Shain's method, the theoretical equations of the potential sweep voltammogram for the ion-transfer with preceding chemical reaction have been numerically calculated. The results are expressed in the form of the working curves for not only the peak current[6)] (i_p) but also the peak potential (E_p) and half-peak potential ($E_{p/2}$) as a function of the kinetic-current parameter of the preceding chemical reaction. Combination of the working curves allows one to elucidate both the rate and equilibrium constants of the chemical reaction.[7)] Thus, the working curves are applied to analyze the potential sweep voltammograms for the transfer of Pb^{2+} ion to nitrobenzene (NB) facilitated by HTCO present in NB from aqueous medium containing citrate^{3-} ion, giving the dissociation and association rate constants as well as the formation constant of Pb^{2+}–citrate^{3-} complex in W-phase.

Theory

We consider the transfer of a metal ion (M) across the O/W interface. When the O-phase contains a hydrophobic ionophore (L, here HTCO), the transfer of M ion (here Pb^{2+} ion) across the O/W interface is facilitated by the formation of a 1 : 1 complex of M with L in O-phase:[1)]

$$M(O) + L(O) \rightleftharpoons ML(O). \qquad (1)$$

We assume (i) that the association and dissociation of ML complex in O-phase (Eq. 1) are very fast processes so that the following Eq. 2 is valid everywhere in O-phase,

$$K^{\mathrm{O}}_{\mathrm{ML}} = c^{\mathrm{O}}_{\mathrm{ML}}/c^{\mathrm{O}}_{\mathrm{M}}c^{\mathrm{O}}_{\mathrm{L}}, \qquad (2)$$

where $K^{\mathrm{O}}_{\mathrm{ML}}$ is the formal formation constant of the ML complex in O-phase and c^{O}_{i} the concentration of i species (i = M, L, and ML) in O-phase. We further assume (ii) that L is so hydrophobic that L and ML species do not transfer across the O/W interface and (iii) that $c^{\mathrm{O}}_{\mathrm{L}}$ is much higher than the total concentration of M ion species in O-phase ($c^{\mathrm{O}}_{\mathrm{M}}+c^{\mathrm{O}}_{\mathrm{ML}}$).

On the other hand, the W-phase contains a hydrophilic ligand (Aw, here citrate^{3-} ion) which associates with M ion to form a 1 : 1 complex:[9]

$$\mathrm{M(W)} + \mathrm{Aw(W)} \rightleftarrows \mathrm{MAw(W)}. \qquad (3)$$

We assume (iv) that the concentration of Aw in W-phase is much higher than the total concentration of M ion species in W-phase. Then, we have

$$\mathrm{M(W)} \underset{k_{\mathrm{b}}^{\mathrm{W}}}{\overset{k_{\mathrm{f}}^{\mathrm{W}\prime}}{\rightleftarrows}} \mathrm{MAw(W)}, \quad K^{\mathrm{W}} = k_{\mathrm{f}}^{\mathrm{W}\prime}/k_{\mathrm{b}}^{\mathrm{W}}, \qquad (4)$$

where $k_{\mathrm{f}}^{\mathrm{W}\prime}$ and $k_{\mathrm{b}}^{\mathrm{W}}$ are the rate constants of the pseudo-monomolecular association and dissociation reactions of MAw complex in W-phase, respectively, and K^{W} is the equilibrium constant. We further assume (v) that Aw is so hydrophilic that Aw and MAw species do not transfer across the O/W interface.

We further assume (vi) that the transfer of M ion species across the O/W interface proceeds according to the mechanism involving the preceding dissociation of MAw to form free M ion which is transferred across the O/W interface. Finally, we assume (vii) that the transfer of M ion across the O/W interface is a very fast process, so that the Nernst–Donnan equation is valid for the partition with respect to the surface concentrations of M ion in W-phase and M ion species in O-phase.

Thus, the facilitated transfer of M ion across the O/W interface in the presence of hydrophilic ligand in W-phase can be studied by assuming the CE-mechanism, that is, the interfacial ion-transfer with preceding chemical reaction. The theory of the potential sweep voltammetry for the case of mechanisms involving a chemical reaction preceding the electron transfer process at the electrode, which is equivalent to the present ion-transfer process, has been well discussed by previous authors.[6—8] Thus, the potential sweep voltammogram exhibits a peak-shaped curve which is characterized by i_{p}, E_{p}, and $E_{\mathrm{p}/2}$. In this study, we adopt the working curve method, in which not only i_{p} but also E_{p} and $E_{\mathrm{p}/2}$ have been calculated as a function of the kinetic-current parameter (λ, see Eq. 8 below), giving the equilibrium constant as well as the rate constants of the preceding chemical reaction.

The calculation was performed under the condition that $lt \gg 1$ ($l = k_{\mathrm{f}}^{\mathrm{W}\prime}+k_{\mathrm{b}}^{\mathrm{W}}$) for the kinetic-current parameter in the range of λ from 0 to 20 at intervals of 0.1. The results are illustrated in Figs. 1 and 2, and are expressed by

$$i_{\mathrm{p}}/{}_{\mathrm{r}}i_{\mathrm{p}} = ((0.472 \pm 0.001)\lambda + 1)^{-1}, \qquad (5)$$

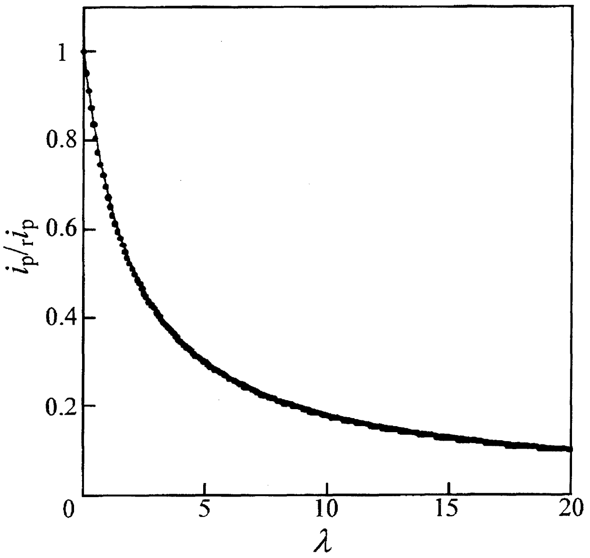

Fig. 1. Plot of $i_{\mathrm{p}}/{}_{\mathrm{r}}i_{\mathrm{p}}$ against λ.

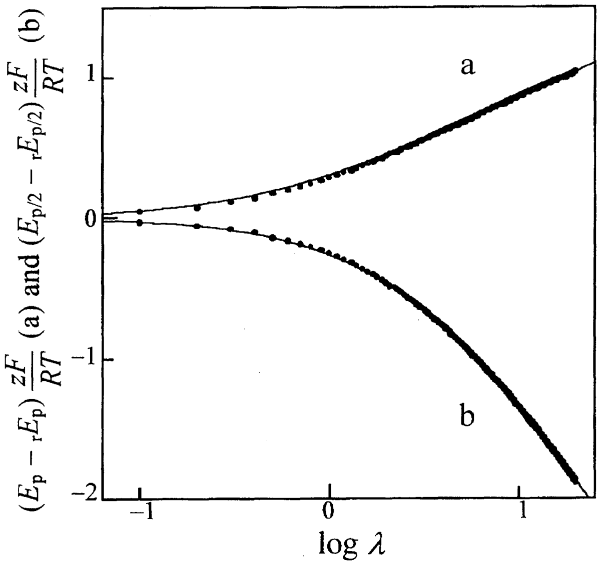

Fig. 2. Plots of a) $(E_{\mathrm{p}} - {}_{\mathrm{r}}E_{\mathrm{p}})(zF/RT)$ and b) $(E_{\mathrm{p}/2} - {}_{\mathrm{r}}E_{\mathrm{p}/2}) \times (zF/RT)$ against log λ.

$$E_{\mathrm{p}} = {}_{\mathrm{r}}E_{\mathrm{p}} + (RT/zF)(0.654 \pm 0.003) \log [1 + (1.900 \pm 0.003)\lambda], \qquad (6)$$

and

$$E_{\mathrm{p}/2} = {}_{\mathrm{r}}E_{\mathrm{p}/2} - (RT/zF)(2.10 \pm 0.01) \log (1 + (0.340 \pm 0.001)\lambda), \qquad (7)$$

with MS_{E} of 2.7×10^{-3}, $(7.5\times10^{-3})(RT/zF)^2$ and $(6.9\times10^{-3})(RT/zF)^2$, respectively, MS_{E} being the mean square error.[11] Equation 5 was first derived by Nicholson and Shain.[6] In these equations, λ is the kinetic-current parameter defined by

$$\lambda = K^{\mathrm{W}} l^{-1/2} a^{1/2}, \qquad (8)$$

with

$$a = (zF/RT)v, \qquad (9)$$

where z is the charge number of M ion, including sign; F,

R, and T are used in the usual meanings; and v is the rate of potential sweep; and ${}_{\rm r}i_{\rm p}$, ${}_{\rm r}E_{\rm p}$, and ${}_{\rm r}E_{\rm p/2}$ are the values of $i_{\rm p}$, $E_{\rm p}$, and $E_{\rm p/2}$ at $\lambda = 0$, that is, the reversible peak current, reversible peak potential, and reversible half-peak potential, given by

$${}_{\rm r}i_{\rm p} = 0.4463 \cdot zFA(D^{\rm W}a)^{1/2}({}^{*}c_{\rm M}^{\rm W})_t, \qquad (10)$$

$${}_{\rm r}E_{\rm p} = {}_{\rm r}E_{1/2} + 1.110 \cdot (RT/zF), \qquad (11)$$

and

$${}_{\rm r}E_{\rm p/2} = {}_{\rm r}E_{1/2} - 1.090 \cdot (RT/zF), \qquad (12)$$

where ${}_{\rm r}E_{1/2}$ is the reversible half-wave potential defined by

$${}_{\rm r}E_{1/2} = E_{\rm M}^{0'} + \frac{RT}{2zF}\ln\frac{D^{\rm W}}{D^{\rm O}} + \frac{RT}{zF}\ln\frac{1+K^{\rm W}}{1+K_{\rm ML}^{\rm O}\,{}^{*}c_{\rm L}^{\rm O}}. \qquad (13)$$

Here, A is the surface area of the O/W interface, $D^{\rm W}$ the common diffusion coefficient of M and MAw in W-phase, $({}^{*}c_{\rm M}^{\rm W})_t$ the total concentration of M ion in the bulk of W-phase, $E_{\rm M}^{0'}$ the formal ion-transfer potential of (simple) M ion across the O/W interface, $D^{\rm O}$ the common diffusion coefficient of M and ML in O-phase, and ${}^{*}c_{\rm L}^{\rm O}$ the bulk concentration of L in O-phase.

Experimental

Facilitated transfer of $\rm Pb^{2+}$ ion by HTCO across the interface between NB and aqueous media was studied by means of linear sweep voltammetry. The electrochemical cell used for the electrochemical measurements can be represented by cell (I) (Chart 1): where TPnACl denotes tetrapentylammonium chloride, TPnATClPB tetrapentylammonium tetrakis[4-chrolophenyl]borate, and $\rm M = mol\,dm^{-3}$. The polarizable NB/W interface, that is, the test interface, is indicated by an asterisk. The applied potential (E) is defined as the terminal potential of the reference electrode RE1 referred to that of RE2, and related to the Galvani potential difference across the O/W interface ($\Delta_{\rm O}^{\rm W}\phi$) by

$$E = \Delta_{\rm O}^{\rm W}\phi + \Delta E_{\rm ref}, \qquad (14)$$

where $\Delta E_{\rm ref}$ is determined by the reference electrode system consisting RE1 and RE2 in cell (I). The reversible half-wave potential of tetramethylammonium ($\rm TMA^+$) ion at the NB/W interface was determined to be 0.369 V by cyclic voltammetry with cell (I), in which phase III is replaced by 0.50 mM TMABr and 0.20 M $\rm LiNO_3$. The standard ion-transfer potential of $\rm TMA^+$ ion is reported to be $\Delta_{\rm O}^{\rm W}\phi_{\rm TMA}^{0} = 0.035$ V.[12] Therefore, on an appropriate assumption,[13] $\Delta E_{\rm ref}$ for cell (I) can be determined to be 0.325 V. $\rm Citrate^{3-}$ ion was added to the test aqueous medium (phase III) as 1 : 2.5 citric acid–LiOH buffer. The ionic strength (I) of the aqueous medium was kept at $I = 0.1$ by addition of $\rm LiNO_3$. The pH of the aqueous medium was determined to be pH = 5.8±0.2. All measurements were carried out at 25±0.5°C. For further details, see Ref. 1.

Results and Discussion

Figure 3 shows linear sweep voltammograms (LSVs) at different bulk concentrations of Aw in W-phase (${}^{*}c_{\rm Aw}^{\rm W}$) for

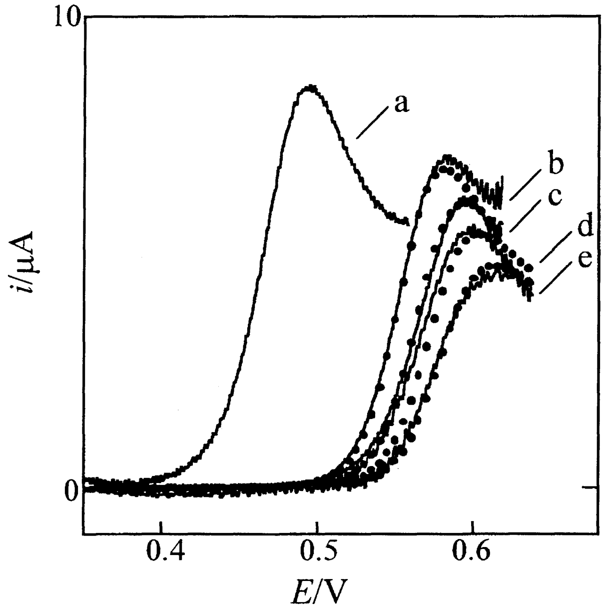

Fig. 3. Linear sweep voltammograms at different concentrations of $\rm citrate^{3-}$ ion, ${}^{*}c_{\rm Aw}^{\rm W}$ = a) 0, b) 1.0, c) 2.5, d) 5.0, and e) 10 mM, for the facilitated transfer of $\rm Pb^{2+}$ ion by HTCO across the NB/W interface, where ${}^{*}c_{\rm L}^{\rm O} = 40$ mM and $({}^{*}c_{\rm M}^{\rm W})_t = 0.10$ mM, and $v = 0.1\ \rm V\,s^{-1}$. The plots are the calculated values on $k_{\rm f}^{\rm W} = 8.0\times10^{10}\ \rm M^{-1}\,s^{-1}$ and $k_{\rm b}^{\rm W} = 4.5\times10^{4}\ \rm s^{-1}$.

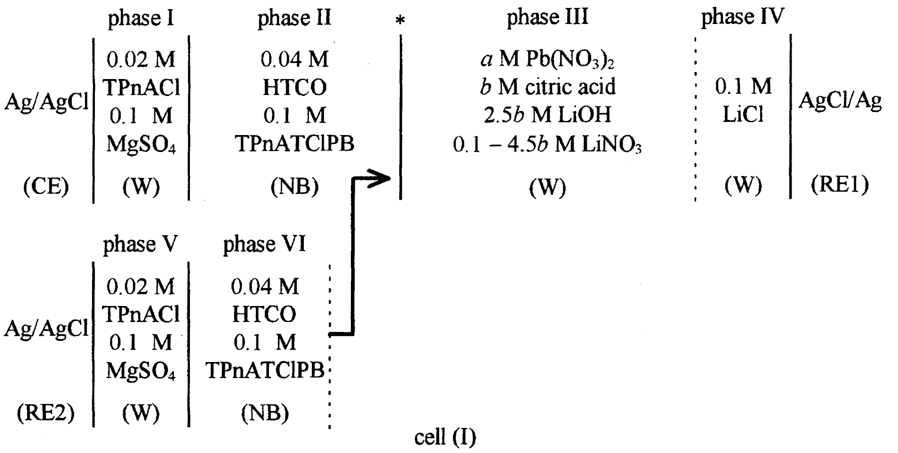

Chart 1.

the facilitated transfer of Pb^{2+} ion by HTCO across the NB/W interface, where $^*c_{\rm L}^{\rm O}=40$ mM, $(^*c_{\rm M}^{\rm W})_t=0.10$ mM, and $^*c_{\rm Aw}^{\rm W}=1.0$—10.0 mM, except curve a where $^*c_{\rm Aw}^{\rm W}=0$, and $v=0.1\ {\rm V\,s^{-1}}$. The LSVs were recorded after correction for the baseline. With increasing $^*c_{\rm Aw}^{\rm W}$, the peak potentials shifted to more positive potential, whereas the peak current height decreased.

In Fig. 4 the observed values of $i_{\rm p}$ are plotted against $v^{1/2}$ at different $^*c_{\rm Aw}^{\rm W}$'s when $(^*c_{\rm M}^{\rm W})_t=0.10$ mM. The voltammetric results at $^*c_{\rm Aw}^{\rm W}=0$ indicate that the facilitated transfer of Pb^{2+} ion by HTCO is reversible and is controlled by the diffusion of Pb^{2+} ionic species in W-phase.[2] Therefore, Eq. 10 was fitted to the plot a in Fig. 4, giving the regression line at $(^*c_{\rm M}^{\rm W})_t=0.10$ mM, as given by

$$({}_{\rm r}i_{\rm p}/\mu{\rm A})=(27.3\pm0.6)(v/{\rm V\,s^{-1}})^{1/2}+(0.0\pm0.2), \qquad (15)$$

with $MS_{\rm E}=0.18\,\mu{\rm A}^2$. Using Eq. 15, Eq. 5 is written by

$$(i_{\rm p}/\mu{\rm A})=[27.3(v/{\rm V\,s^{-1}})^{1/2}]/[(4.17\ {\rm V^{-1/2}})(\lambda a^{-1/2}/{\rm s^{1/2}})(v/{\rm V\,s^{-1}})^{1/2}+1], \qquad (16)$$

where $a=(zF/RT)v$ with $zF/RT=77.9\ {\rm V^{-1}}$ is employed. Equation 16 was fitted to plots b—f in Fig. 4. The 90% confidence limits on the mean value of $\lambda a^{-1/2}(=K^{\rm W}l^{-1/2})$ were determined to be 0.14±0.02, 0.22±0.02, 0.27±0.03, 0.47±0.02, and 0.62±0.03 s$^{1/2}$ for $^*c_{\rm Aw}^{\rm W}=0.5$, 1.0, 2.5, 5.0, and 10 mM, respectively. The solid lines in Fig. 4 are the regression curves on these $K^{\rm W}l^{-1/2}$ values. Another possible mechanism to interpret the present voltammetric behavior would be the mechanism involving the rate-determining interfacial ion-transfer combined with the very fast chemical reactions in both O- and W-phases (similar to the chemical reaction in O-phase of Eqs. 1 and 2), in which, however, as the theory predicts,[10] the dependence of $i_{\rm p}/{}_{\rm r}i_{\rm p}$ on a kinetic parameter should not be expressed by an equation similar in form to Eq. 5 in the range of the parameters tested in this study. Further experimental evidence to support the assumed mechanism can be obtained by potential-step chronoamperometric study,[14] which will be published in a succeeding paper.

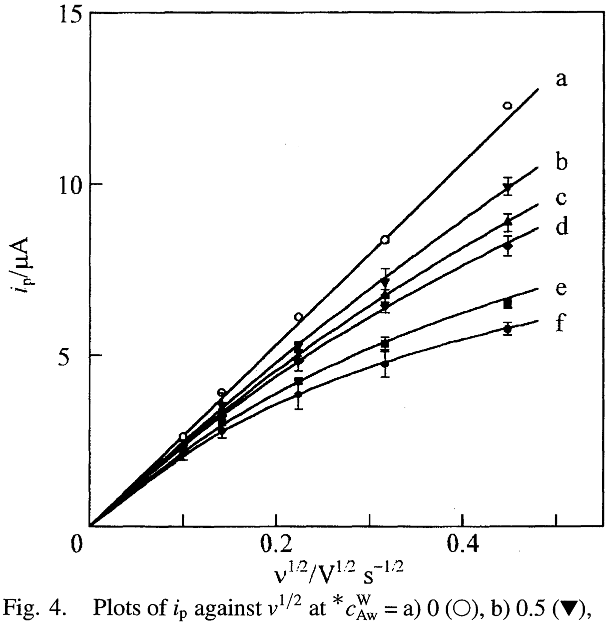

Fig. 4. Plots of $i_{\rm p}$ against $v^{1/2}$ at $^*c_{\rm Aw}^{\rm W}$ = a) 0 (○), b) 0.5 (▼), c) 1.0 (▲), d) 2.5 (◆), e) 5.0 (■), and f) 10 (●) mM, and at $(^*c_{\rm M}^{\rm W})_t=0.10$ mM. Vertical bars indicate the standard deviations (usually, $n=5$).

Let the second-order rate constant of the association reaction of MAw complex in W-phase (Eq. 3) be $k_{\rm f}^{\rm W}$. We define the formal formation constant of the MAw complex in W phase ($K_{\rm MAw}^{\rm W}$) by

$$K_{\rm MAw}^{\rm W}=k_{\rm f}^{\rm W}/k_{\rm b}^{\rm W}. \qquad (17)$$

On the assumption that the complex formation of Pb^{2+} ion with citrate^{3-} ion in the aqueous medium is largely shifted to the complex side, that is, $K^{\rm W}=K_{\rm MAw}^{\rm W}\,{}^*c_{\rm Aw}^{\rm W}\gg1$ (see below), the measured values of $\lambda a^{-1/2}$ can be approximated by

$$\lambda a^{-1/2}=(K_{\rm MAw}^{\rm W}(k_{\rm f}^{\rm W})^{-1/2})(^*c_{\rm Aw}^{\rm W})^{1/2}. \qquad (18)$$

In Fig. 5 the measured values of $\lambda a^{-1/2}$ are plotted against $(^*c_{\rm Aw}^{\rm W})^{1/2}$. The regression line fitted to the plot is expressed by

$$(\lambda a^{-1/2}/{\rm s^{1/2}})=(6.3\pm1.1)(^*c_{\rm Aw}^{\rm W}/{\rm M})^{1/2}+(0.02\pm0.07), \qquad (19)$$

with $MS_{\rm E}=8.5\times10^{-4}$ s, which is shown by the solid line in Fig. 5, giving $K_{\rm MAw}^{\rm W}(k_{\rm f}^{\rm W})^{-1/2}=6.3\pm1.1\ {\rm M^{-1/2}\,s^{1/2}}$.

The experimental values of $E_{\rm p}$ and $E_{\rm p/2}$ observed at $v=0.01\ {\rm V\,s^{-1}}$ are plotted against $\log{}^*c_{\rm Aw}^{\rm W}$, on plots a and b in Fig. 6, respectively. The values of ${}_{\rm r}E_{\rm p}$ and ${}_{\rm r}E_{\rm p/2}$ can be calculated by Eqs. 6 and 7 from the observed values of $E_{\rm p}$ and $E_{\rm p/2}$, respectively, where $\lambda=(K_{\rm MAw}^{\rm W}(k_{\rm f}^{\rm W})^{-1/2})a^{1/2}(^*c_{\rm Aw}^{\rm W})^{1/2}=(6.3\ {\rm M^{-1/2}\,s^{1/2}})\times(0.883\ {\rm s^{-1/2}})\times(^*c_{\rm Aw}^{\rm W}/{\rm M})^{1/2}$ can be used (see above). The calculated values of ${}_{\rm r}E_{\rm p}$ and ${}_{\rm r}E_{\rm p/2}$ are also plotted against $\log{}^*c_{\rm Aw}^{\rm W}$ on plots c and d in Fig. 6, respectively. By combination of Eq. 13 with Eqs. 11 and 12 under the

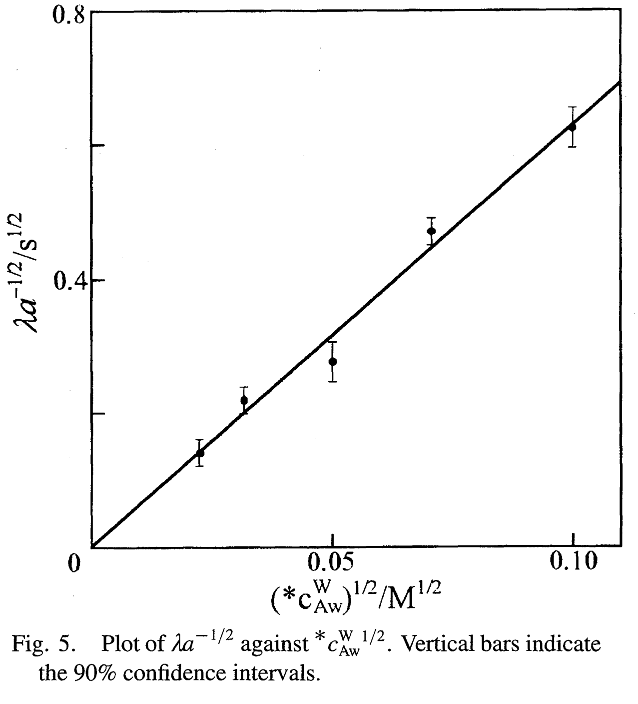

Fig. 5. Plot of $\lambda a^{-1/2}$ against $^*c_{\rm Aw}^{\rm W\,1/2}$. Vertical bars indicate the 90% confidence intervals.

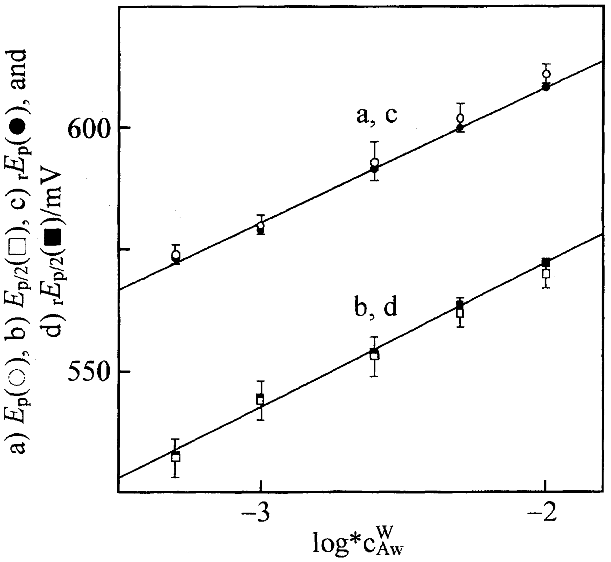

Fig. 6. Plots of the observed values of a) E_p and b) $E_{p/2}$, with error bars indicating the 90% confidence intervals, at $v = 0.01$ V s^{-1} and the calculated values of c) $_rE_p$ and d) $_rE_{p/2}$ by Eqs. 6 and 7 (see text) against $\log {}^*c_{Aw}^W$.

assumption that $K^W = K_{MAw}^W {}^*c_{Aw}^W \gg 1$ (see below), $_rE_p$ and $_rE_{p/2}$ can be expressed, respectively, by

$$_rE_p = {}_rE_{p,M/ML} + (RT/zF)\ln K_{MAw}^W + (RT/zF)\ln {}^*c_{Aw}^W \tag{20}$$

and

$$_rE_{p/2} = {}_rE_{p/2,M/ML} + (RT/zF)\ln K_{MAw}^W + (RT/zF)\ln {}^*c_{Aw}^W, \tag{21}$$

where $_rE_{p,M/ML}$ and $_rE_{p/2,M/ML}$ are the reversible peak potential and the reversible half-peak potential at ${}^*c_{Aw}^W = 0$. Thus, the plots c and d are fitted to the regression lines, which are expressed by

$$_rE_p/\text{mV} = (664 \pm 7) + (28 \pm 2)\log {}^*c_{Aw}^W \tag{22}$$

and

$$_rE_{p/2}/\text{mV} = (631 \pm 9) + (30 \pm 3)\log {}^*c_{Aw}^W, \tag{23}$$

with MS_E of 1.2 and 2.0 mV^2, respectively. These regression lines are shown by solid lines in Fig. 6. Thus, $\log K_{MAw}^W$ was determined to be $6.2_5 \pm 0.2$ from the $_rE_p$ plot and 6.1 ± 0.3 from the $_rE_{p/2}$ plot, where the observed value of $E_p = 479$ mV and $E_{p/2} = 450$ mV at ${}^*c_{Aw}^W = 0$ were used for $_rE_{p,M/ML}$ and $_rE_{p/2,M/ML}$, respectively. These $\log K_{MAw}^W$ values are in harmony with each other and with the value of 6.50 reported by potentiometry with Pb electrode.[9] Also, note that $K_{MAw}^W {}^*c_{Aw}^W \gg 1$. In the present study, a nitrate medium was used, although Pb^{2+} ion is known to form a 1 : 1 complex with NO_3^- ion ($PbNO_3^+$). The formal formation constant of $PbNO_3^+$ (K_{PbNO3}^W) in aqueous media can be calculated to be $10^{0.60}$ M^{-1} at $I = 0.1$.[15] Since $K_{MAw}^W {}^*c_{Aw}^W \gg K_{PbNO3}^W(0.1\ \text{M} - 9\times{}^*c_{Aw}^W)$ in the range of ${}^*c_{Aw}^W$ from 0.50 to 10.0 mM, the complex formation of $PbNO_3^+$ in the aqueous medium can be neglected.

Using $K_{MAw}^W (k_f^W)^{-1/2} = 6.3 \pm 1.1$ M$^{-1/2}$ s$^{1/2}$ and $\log K_{MAw}^W = 6.2_5 \pm 0.2$, the 90% confidence limits on the mean values of k_f^W and k_b^W for 1 : 1 Pb^{2+}–citrate^{3-} complex can be calculated to be $(8._0 \pm 7._3)\times 10^{10}$ M^{-1} s^{-1} and $(4._5 \pm 2._5)\times 10^4$ s^{-1}, respectively. The k_f^W is in the order of the rate constants for a diffusion-controlled bimolecular reaction.[16] Finally, LSVs calculated on these rate constants are plotted in Fig. 3. The calculated voltammograms are in fair agreement with the experimental ones.

This paper is the first report, to the authors' knowledge, on the preceding chemical reaction-controlled ion-transfer current at liquid/liquid interface, which can be exactly analyzed using potential sweep voltammetry. This study also shows that combinations of the working curve for the peak current as a function of the kinetic-current parameter with those for the peak potential and/or the half-peak potential are useful to determine the association and dissociation rate constants and the formation constant of the preceding chemical reaction.

The work was supported by Grants-in-Aid for Scientific Research from Fukui-ken University Science Foundation, to which the authors (M.S. and H.K.) are very grateful, and also by a Grant-in-Aid for Scientific Research No. 9740560 from the Ministry of Education, Science, and Culture, to which the author (H. K.) is very grateful.

References

1) H. Katano and M. Senda, *Anal. Sci.*, **12**, 683 (1996).
2) H. Katano and M. Senda, *Bull. Chem. Soc. Jpn.*, **70**, 2489 (1997).
3) H. Katano, K. Tanaka, and M. Senda, *Anal. Sci.*, **13S**, 299 (1997).
4) a) J. Heyrovský and Kuta, "Principles of Polarography," Academic Press, New York (1966), p. 339; b) P. Delahay, "New Instrumental Methods in Electrochemistry," Interscience Publishers Inc., New York (1954), p. 87.
5) T. Kakutani, Y. Nishiwaki, T. Osakai, and M. Senda, *Bull. Chem. Soc. Jpn.*, **59**, 781 (1986).
6) R. S. Nicholson and I. Shain, *Anal. Chem.*, **36**, 706 (1964).
7) J. M. Savéant and F. Xu, *J. Electroanal. Chem.*, **208**, 197 (1986).
8) M. Rudolph, D. P. Reddy, and S. W. Feldberg, *Anal. Chem.*, **66**, 581 (1994), and papers cited therein.
9) S. S. Kety, *J. Biol. Chem.*, **142**, 181 (1942).
10) H. Matsuda and Y. Ayabe, *Z. Elektrochem.*, **59**, 494 (1955).
11) D. C. Montgomery and G. C. Runger, "Applied Statistics and Probability for Engineers," John Wiley and Sons, New York (1994), p. 554.
12) J. Koryta, P. Vanýsek, and M. Brezina, *J. Electroanal. Chem.*, **75**, 211 (1977).
13) T. Kakutani, T. Osakai, and M. Senda, *Bull. Chem. Soc. Jpn.*, **56**, 991 (1983).
14) H. Katano and M. Senda, unpublished resutls.
15) R. A. Robinson and R. H. Stokes, "Electrolyte Solutions," Butterworth, London (1959), p. 232.
16) P. Debye, *Trans. Electrochem. Soc.*, **82**, 265 (1942).